Catalysis Communications 51 (2014) 58–62

Contents lists available at ScienceDirect

Catalysis Communications

journal homepage: www.elsevier.com/locate/catcom

Short Communication

Mo_2N nanobelts for dehydrogenation of aromatic alcohols

Zhongcheng Li [a,b], Chunhui Chen [a], Ensheng Zhan [a], Na Ta [a], Wenjie Shen [a,*]

[a] State Key Laboratory of Catalysis, Dalian Institute of Chemical Physics, Chinese Academy of Sciences, Dalian 116023, China
[b] University of Chinese Academy of Sciences, Beijing 100049, China

ARTICLE INFO

Article history:
Received 12 February 2014
Received in revised form 20 March 2014
Accepted 23 March 2014
Available online 28 March 2014

Keywords:
Mo_2N
Nanobelts
Aromatic alcohols
Dehydrogenation

ABSTRACT

Mo_2N nanobelts about 60 nm wide and 0.5–7.2 μm long have been synthesized by reacting a belt-shaped α-MoO_3 precursor with ammonia at 850 °C. The Mo_2N nanobelts effectively and selectively catalyzed dehydrogenation of a variety of aromatic alcohols. The coordinatively unsaturated Mo sites on the surface of the Mo_2N nanobelts might be the active species.

1. Introduction

Non-oxidative dehydrogenation of alcohols to aldehydes or ketones has been viewed as an important route in alcohol transformation with the characters of higher atom efficiency and better selectivity; precious metal nanoparticles such as Au [1,2], Ag [3,4], Ru [5] and Pt [6], have been reported to be highly active for this process. However, the high price and limited availability of these precious metals have hampered the widespread application of the process to some extents. In this respect, design and development of less expensive but efficient catalysts for the non-oxidative dehydrogenation of alcohols are highly expected. Molybdenum nitrides were reported to show similar catalytic property to precious metals in pyridine hydrodenitrogenation [7], *p*-chloronitrobenzene hydrogenation [8], n-butane dehydrogenation [9] and NH_3 synthesis and decomposition [10,11]. This was ascribed to the similar electronic feature of molybdenum nitrides to that of precious metals; the incorporation of nitrogen atoms into the lattice of Mo atoms expended the Mo – Mo bond distance and increased the density of states at the Fermi level of the Mo atom [12,13].

The catalytic property of molybdenum nitrides is closely associated with their size and shape. The main procedures for preparing molybdenum nitrides included nitridation of metallic Mo with N_2 [14], pyrolysis of Mo–organic complexes [15], and nitridation of MoO_3 with ammonia or N_2/H_2 mixtures at elevated temperatures [16,17]. In most cases, the resulting molybdenum nitrides had wide size distributions and irregular shapes; their sizes are usually in the range of micrometers while their shapes are often spherical or irregular in bulky form. Tailoring the size and shape of molybdenum nitrides has attracted wide attention in recent years; significant progress has been achieved in lowering the size to the nanometer level and mediating the morphology into one-dimensional nanostructures. For example, Mo_2N particles of 20–40 nm were synthesized by pyrolysis of a $MoCl_5$–urea mixture at 800 °C under nitrogen atmosphere [18]. Mo_2N nanofibers and nanowires were obtained through nitridation of α-MoO_3 precursors with ammonia at high temperatures [19,20]. Topotactical nitridation of α-MoO_3 fibers with ammonia at 785 °C produced Mo_2N fibers with a diameter of about 300 nm and a length of up to several micrometers [19]. Reaction of α-MoO_3 nanowires with NH_3 at 700 °C yielded molybdenum nitride nanowires [20]. However, these nanostructured molybdenum nitrides still had relatively large sizes and non-uniform distributions; the simultaneous control of size and shape of molybdenum nitrides at the nanometer level is scarcely reported.

We have recently synthesized well-defined α-MoO_3 nanobelts using a hydrothermal method [21]. In this work, we extended to prepare small-sized Mo_2N nanobelts by treating the belt-shaped α-MoO_3 precursor with ammonia at 850 °C. The resulting Mo_2N nanobelts had an average width of about 60 nm and lengths of 0.5–7.2 μm, and effectively catalyzed dehydrogenation of a variety of aromatic alcohols to the corresponding aldehydes or ketones.

2. Experimental

2.1. Catalyst preparation

The α-MoO_3 nanobelts, 8 nm thick, 60 nm wide, and 0.7–7.5 μm long, were synthesized using a hydrothermal method [21]. The molybdenum nitride nanobelts were prepared by treating the belt-shaped MoO_3 precursor with ammonia at 850 °C. 100 mg α-MoO_3 nanobelts were heated to 200 °C at a rate of 5 °C/min under N_2 flow (30 ml/min) and

* Corresponding author. Fax: +86 411 84694447.
E-mail address: shen98@dicp.ac.cn (W. Shen).

http://dx.doi.org/10.1016/j.catcom.2014.03.029
1566-7367/

maintained at that temperature for 1 h. Then, the sample was exposed to NH_3 (50 ml/min), heated to 850 °C at a rate of 1 °C/min, and maintained at that temperature for 4 h. After being cooled down to room temperature, the sample was passivated with a 1% O_2/N_2 mixture (30 ml/min) for 4 h before it was exposed to air.

2.2. Catalyst characterization

The X-ray diffraction (XRD) patterns were collected on a Rigaku D/Max2500V/PC powder diffractometer with a Cu Kα radiation source (40 kV, 100 mA).

The nitrogen adsorption–desorption isotherms were measured on a Nova 4200e instrument at −196 °C. Before the measurement, the sample was degassed at 300 °C for 6 h under vacuum. The specific surface area was calculated by a multipoint Brunauer–Emmett–Teller method. The transmission electron microscopy (TEM) images were recorded on a Philips Tecnai G^2 Spirit microscope (120 kV). The high-resolution TEM (HRTEM) images were taken on a FEI Tecnai G^2 F30 Spirit microscope (300 kV). The specimen was prepared by ultrasonically dispersing the sample into ethanol, depositing droplets of the suspensions onto a carbon-enhanced copper grid, and drying them in air. The field-emission scanning electron microscopy (FESEM) images were taken on a Philips Fei Quanta 200F instrument operated at 20 kV. The sample was placed on a conductive carbon tape adhered to an aluminum sample holder.

The X-ray photoelectron spectroscopy (XPS) was performed with a VG ESCALAB MK2 spectrometer using an Al Kα radiation source operated at an accelerating voltage of 12.5 kV. The passivated sample was pressed into thin discs and mounted on a sample rod placed in the analysis chamber. Before the test, the sample was pre-treated with hydrogen at 500 °C for 3 h to regenerate the molybdenum nitrides. The charging effect was corrected by adjusting the binding energy of C1s to 284.5 eV. To determine the distribution of molybdenum species at different oxidation states, the Mo 3d spectrum was deconvoluted using a XPSPEAK program with a combined Gaussian–Lorentzian function. The bind energies of Mo $3d_{5/2}$ and Mo $3d_{3/2}$ were separated by 3.2 eV with a peak area ratio of 3/2. The binding energies of Mo $3d_{5/2}$ were set as follows: Mo^0 (227.6 eV), Mo^{2+} (228.3 eV), Mo^{4+} (229.6 eV), Mo^{5+} (231.4 eV) and Mo^{6+} (232.7 eV) [22,23].

2.3. Catalytic test

The dehydrogenation of alcohols was performed in a 10 ml 2-neck flask equipped with a reflux condenser under N_2 atmosphere. The fresh Mo_2N nanobelts (60 mg) were liquid-sealed by dimethyl sulfoxide under nitrogen flow and quickly transferred into the flask. 1 mmol alcohol was added into the flask containing 4 ml dimethyl sulfoxide and the catalyst. The reaction mixture was heated to 150 °C and maintained at that temperature for a certain period. After reaction, the liquid product was collected by centrifugation and analyzed by an Agilent GC-7890 gas chromatography equipped with a HP-5 capillary column. For the recycle test, the catalyst was immersed in dimethyl sulfoxide to avoid its exposure to air.

3. Results and discussion

Fig. 1 shows the XRD pattern and SEM/TEM images of the Mo_2N nanobelts. The sample exhibited characteristic diffraction lines of face-centered cubic γ-Mo_2N (JCPDS#25-1366), and had a width of about 60 nm and lengths of 0.5–7.2 μm, inheriting the size and shape of the

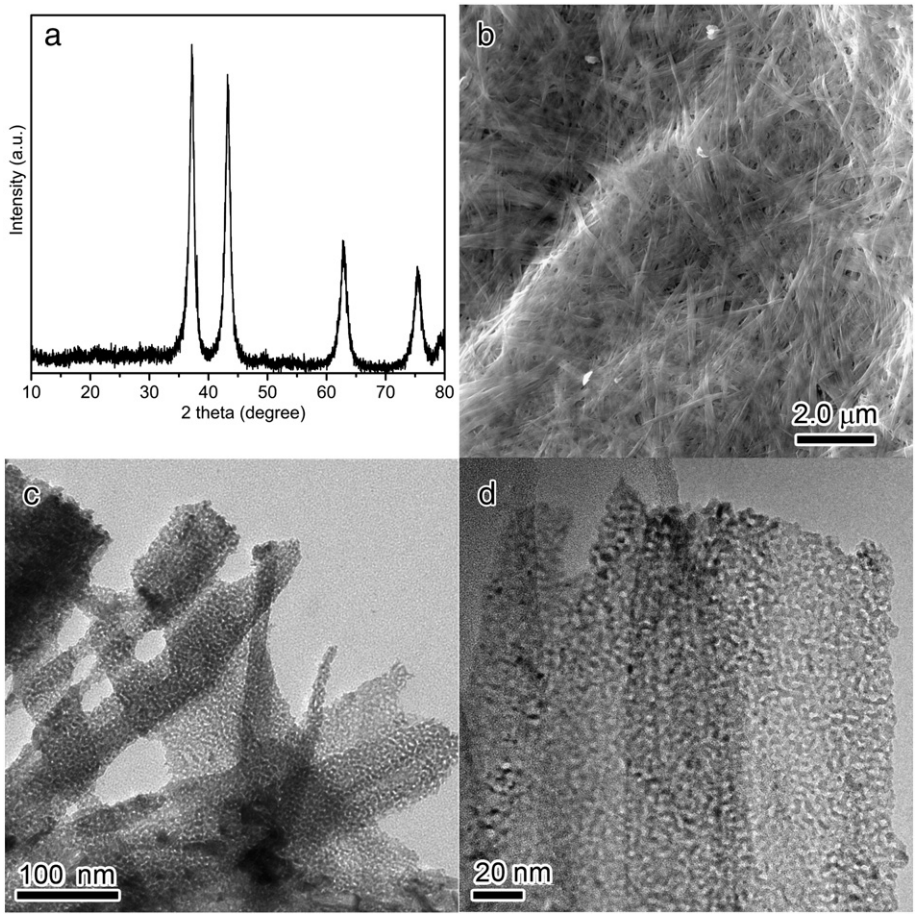

Fig. 1. XRD pattern (a) and SEM/TEM images (b–d) of the Mo_2N nanobelts.

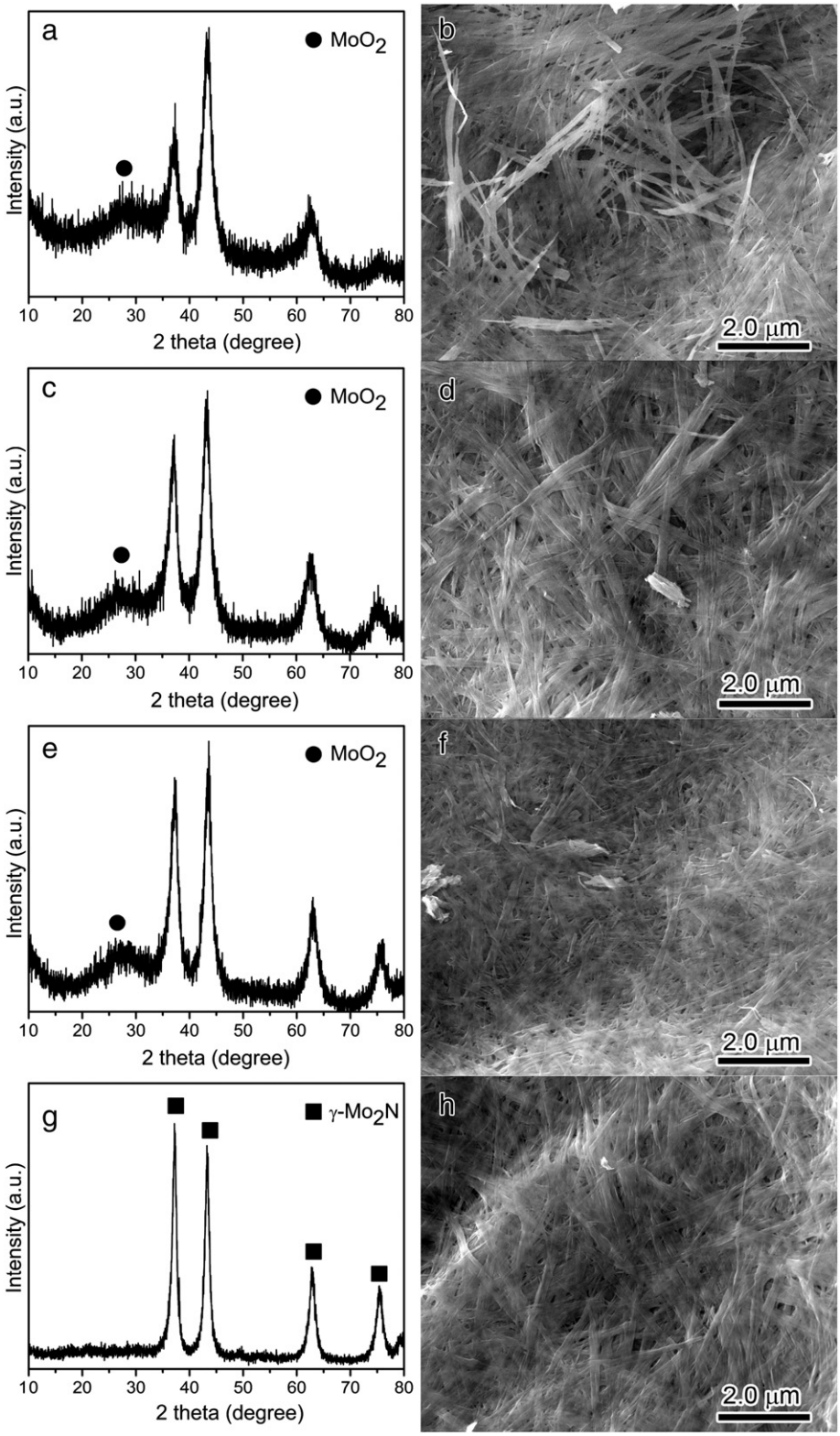

Fig. 2. XRD patterns and SEM images of the products obtained during the nitridation of the α-MoO_3 precursor with ammonia at (a, b) 550 °C, (c, d) 650 °C, (e, f) 750 °C and (g, h) 850 °C for 4 h.

α-MoO_3 precursor [21]. The Mo_2N nanobelts also had appreciable amounts of pores with a size of about 1.6 nm, which were generated during the reaction between MoO_3 and NH_3. Nitrogen atom is incorporated into the lattice of molybdenum while hydrogen atom is combined with the lattice oxygen to form water [19]. Since the oxygen vacancies may not be completely occupied and compensated by nitrogen atoms, micropores were generated at the framework of the resulting molybdenum nitride [20]. As a consequence, the Mo_2N nanobelts had a much higher surface area (85.9 m^2/g) than the α-MoO_3 precursor (25.6 m^2/g) [21].

The formation of the Mo_2N nanobelts strongly depended on the temperature of nitridation. As shown in Fig. 2, the reaction of the α-MoO_3 precursor with NH_3 readily started at 550 °C, but formed a mixture of Mo_2N and MoO_2. At 650–750 °C, the intensities of the diffraction

lines of Mo_2N substantially enhanced, indicating the improved crystallinity. However, minor diffraction lines of MoO_2 were still observed probably due to the slow diffusion of nitrogen atoms into the lattice of molybdenum oxides. At 850 °C, the diffraction lines of MoO_2 entirely disappeared and these of Mo_2N solely presented. These results evidence that the transformation of α-MoO_3 to Mo_2N through a partially reduced MoO_2-like intermediate and a higher temperature up to 850 °C may be required to produce pure Mo_2N. The Mo_2N nanobelts had a width of about 60 nm and lengths of 0.5–7.2 μm in the temperature range examined, similar to the belt-shaped α-MoO_3 precursor. This observation is consistent with previous studies on the evolutions of crystal phase and morphology during nitridation of MoO_3 with ammonia [16,24]. For example, MoO_2 and Mo_2N were simultaneously formed at 500–600 °C, whereas Mo_2N was exclusively produced only at 700 °C [16]. Nitridation of MoO_3 or $(NH_4)_6Mo_7O_{24}\cdot 4H_2O$ with ammonia at 625–750 °C produced molybdenum nitrides, but their size and morphology were closely related with the molybdenum precursor. It is generally believed that such a pseudomorphic transformation involved a reaction mechanism in which the molybdenum atoms are constrained [24]. Here, similar phase transformation was observed during the nitridation of the belt-shaped α-MoO_3 precursor with ammonia, in which the MoO_2-like compound acted as the key intermediate for the formation of the face-centered cubic molybdenum nitrides.

Fig. 3 shows the XPS profile of Mo 3d in the Mo_2N nanobelts. The percentage of surface Mo^{2+}, Mo^{4+}, and Mo^{5+} species was up to 74.2%, suggesting that these coordinatively unsaturated molybdenum species are predominant on the surface of the Mo_2N nanobelts. This is quite similar to the early observations on bulky molybdenum nitrites. The dominant molybdenum species on a Mo_2N sample (4 m^2/g) were Mo^{2+} (57%) and Mo^{4+} (29%) [7]. Another Mo_2N sample (140 m^2/g) presented Mo^{2+} (70%) and Mo^{4+} (23%) species on its surface [16].

The Mo_2N nanobelts effectively catalyzed dehydrogenation of benzyl alcohol with >99% selectivity towards benzaldehyde. As listed in Table 1, the conversion of benzyl alcohol, on the Mo_2N nanobelts, was 32% within 24 h at 120 °C. As the temperature was raised to 150 °C, the conversion of benzyl alcohol reached 18% at 2 h, gradually increased over time, and approached 100% at 28 h. A blank test without the use of catalyst did not produce any benzaldehyde, indicating the heterogeneous catalysis nature of the reaction. Recycle tests verified that the Mo_2N nanobelts retained stable activity and selectivity for three consecutive runs, demonstrating that the Mo_2N nanobelts are a promising catalyst for the dehydrogenation of benzyl alcohol.

The Mo_2N nanobelts were also active for the dehydrogenation of other types of aromatic alcohols. As shown in Table 2, dehydrogenation of 4-methoxybenzyl alcohol exclusively produced 4-methoxybenzyl aldehyde; the conversion of the substrate reached 100% at 21 h. It seems that these electron-donating groups in the benzyl ring of the alcohols favored a relatively higher dehydrogenation activity on the Mo_2N nanobelts. For comparison, dehydrogenation of other alcohols was also tested. Secondary aromatic alcohol, 1-phenylethanol, was dehydrogenated to acetophenone with a yield of 45% at 2 h and 100% at 24 h. In the case of cycloaliphatic alcohols, like cyclohexylmethanol, however, the yield of cycloaldehyde was only 11% within 24 h. However, the Mo_2N nanobelts showed lower activities in the dehydrogenation of secondary aliphatic alcohols like 2-octanol. The reaction proceeded very slowly and the conversion of 2-octanol was only 6% at 24 h. All these results evidenced that the Mo_2N nanobelts were more active for the dehydrogenation of aromatic alcohols, but much less active for aliphatic alcohols.

To date, only a few heterogeneous catalysts, mostly precious metal nanoparticles, have been demonstrated to be highly active for the non-oxidative dehydrogenation of alcohols, but their selectivities towards the desired products strongly depended on the acid–base properties of the oxide-support. For example, Au nanoparticles supported on a verity of oxides offered 2.1–89% conversion of benzyl alcohol and 49–99% selectivity towards benzaldehyde at 120 °C for 6 h; hydrotalcite-supported gold catalysts provided the highest activity and selectivity in the non-oxidative dehydrogenation of alcohols [2]. The superior performance was primarily ascribed to the basic sites on the hydrotalcite, which extracted a proton from the hydroxyl group of alcohol and then underwent α-hydride elimination to yield the carbonyl product [25]. Ag nanoparticles on alumina were also active for the dehydrogenation of alcohols; but the yields of aldehydes varied largely from 16% to 94%; the Al_2O_3 support provided basic sites for the abstraction proton from alcohol and acidic sites for the release of hydrogen, while the silver site was responsible for the dissociation of the C–H bond [4]. Pt nanoclusters on Al_2O_3 were highly active for the dehydrogenation of

Table 1
Reaction results of dehydrogenation of benzyl alcohol on the Mo_2N nanobelts.

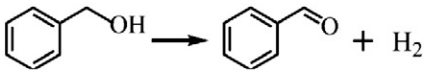

Entry	Temperature (°C)	Time (h)	Conversion (%)
1	120	24	32
2	150	2	18
3	150	4	25
4	150	6	32
5	150	12	52
6	150	24	90
7	150	28	100
Resue 1	150	28	100
Reuse 2	150	28	100
8[a]	150	24	–

Reaction conditions: 1 mmol benzyl alcohol, 4 ml dimethyl sulfoxide, and 60 mg catalyst.
[a] Blank test without the use of catalyst.

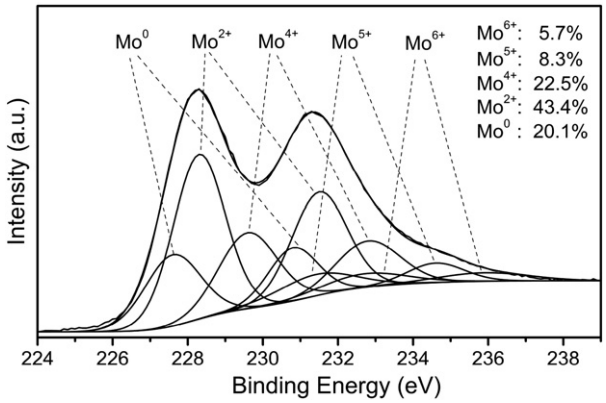

Fig. 3. XPS profile of Mo 3d in the Mo_2N nanobelts.

Table 2
Reaction results of dehydrogenations of alcohols on the Mo_2N nanobelts.

Substrate	Product	Time (h)	Conversion (%)
4-Methoxybenzyl alcohol	4-Methoxybenzyl aldehyde	2	26
		4	38
		6	49
		20	100
4-Methybenzyl alcohol	4-Methybenzyl aldehyde	2	20
		4	34
		6	44
		21	100
1-Phenylethanol	Acetophenone	2	45
		24	100
Cyclohexylmethanol	Cyclohexanecarboxaldehyde	24	11
2-Octanol	2-Octanone	24	6

Reaction conditions: 1 mmol alcohol, 4 ml dimethyl sulfoxide, 60 mg catalyst, and 150 °C.

aliphatic alcohols, providing 78–97% yields of aldehydes/ketones at 130–180 °C within 48–90 h; the activity for dehydrogenation of 2-octanol was closely associated with the acid–base character of the support, and amphoteric support exhibited a higher activity than acidic and basic ones [6]. Although molybdenum nitrides have been less studied in the dehydrogenation of alcohols, the reaction results obtained on the current Mo_2N nanobelts demonstrate that they might be a potential alternative to noble metals in terms of the high selectivity and the reasonable activity. It was previously proposed that the coordinatively unsaturated surface Mo sites on a Mo_2N/Al_2O_3 catalyst, probed by CO absorption, accounted for the high activity in hydrodesulfurization of thiophene, in which the bonding between thiophene through its sulfur atom and the surface coordinated unsaturated Mo site activated the C–S bond; the N site may not be directly involved in the catalytic reaction but they modified the electronic properties of the Mo site [26,27]. Isomerization of 1-butene to 2-butene was also suggested to occur on the coordinatively unsaturated Mo sites of a Mo_2N/Al_2O_3 catalyst [28]. Therefore, it is most likely that the coordinatively unsaturated molybdenum sites (74.2%) on the Mo_2N nanobelts accounted for the activity in the dehydrogenation of benzyl alcohols. First, the O–H bond of benzyl alcohol was activated by the electron-rich $N^{\delta-}$ site to yield the alkoxide group and a proton. Then, the cleavage of the C–H bond in the alkoxide intermediate occurred on the coordinatively unsaturated $Mo^{\delta+}$ site, forming benzaldehyde and a hydride specie. Combination of the hydride specie on the $Mo^{\delta+}$ site with the proton on the $N^{\delta-}$ site generated a hydrogen molecule that was released from the catalyst surface.

4. Conclusions

Mo_2N nanobelts about 60 nm wide and 0.5–7.2 μm long have been synthesized through temperature-programmed nitridation of a belt-shaped α-MoO_3 precursor with ammonia. The Mo_2N nanobelts were highly selective for the dehydrogenation of aromatic alcohols, primarily due to the presence of appreciable amounts of coordinatively unsaturated molybdenum species on the surface.

Acknowledgment

We gratefully acknowledge the financial support for this research work from the National Key Basic Research Program of China (2013CB933100) and the National Natural Science Foundation of China (21103177).

References

[1] W.H. Fang, Q.H. Zhang, J. Chen, W.P. Deng, Y. Wang, Chem. Commun. 46 (2010) 1547–1549.
[2] W.H. Fang, J.S. Chen, Q.H. Zhang, W.P. Deng, Y. Wang, Chem. Eur. J. 17 (2011) 1247–1256.
[3] T. Mitsudome, Y. Mikami, H. Funai, T. Mizugaki, K. Jitsukawa, K. Kaneda, Angew. Chem. Int. Ed. 47 (2008) 138–141.
[4] K. Shimizu, K. Sugino, K. Sawabe, A. Satsuma, Chem. Eur. J. 15 (2009) 2341–2351.
[5] B. Feng, C. Chen, H.M. Yang, X.G. Zhao, L. Hua, Y.Y. Yu, T. Cao, Y. Shi, Z.S. Hou, Adv. Synth. Catal. 354 (2012) 1559–1565.
[6] K. Kon, S. Siddiki, K.I. Shimizu, J. Catal. 304 (2013) 63–71.
[7] J.G. Choi, J.R. Brenner, C.W. Colling, B.G. Demczyk, J.L. Dunning, L.T. Thompson, Catal. Today 15 (1992) 201–222.
[8] F. Cárdenas-Lizana, S. Gómez-Quero, N. Perret, L. Kiwi-Minsker, M.A. Keane, Catal. Sci. Technol. 1 (2011) 794–801.
[9] M.K. Neylon, S. Choi, H. Kwon, K.E. Curry, L.T. Thompson, Appl. Catal. A 183 (1999) 253–263.
[10] D. McKay, J.S.J. Hargreaves, J.L. Rico, J.L. Rivera, X.L. Sun, J. Solid State Chem. 181 (2008) 325–333.
[11] W. Zheng, T.P. Cotter, P. Kaghazchi, T. Jacob, B. Frank, K. Schlichte, W. Zhang, D.S. Su, F. Schüth, R. Schlögl, J. Am. Chem. Soc. 135 (2013) 3458–3464.
[12] S.T. Oyama, Catal. Today 15 (1992) 179–200.
[13] S.W. Yang, Y.X. Li, C.X. Ji, C. Li, Q. Xin, J. Catal. 174 (1998) 34–42.
[14] X.Z. Chen, J.L. Dye, H.A. Eick, S.H. Elder, K.L. Tsai, Chem. Mater. 9 (1997) 1172–1176.
[15] N.A.K. Hansen, W.A. Herrmann, Chem. Mater. 10 (1998) 1677–1679.
[16] Y.J. Zhang, Q. Xin, I. Rodriguez-Ramos, A. Guerrero-Ruiz, Mater. Res. Bull. 34 (1999) 145–156.
[17] F. Cárdenas-Lizana, D. Lamey, S. Gómez-Quero, N. Perret, L. Kiwi-Minsker, M.A. Keane, Catal. Today 173 (2011) 53–61.
[18] C. Giordano, C. Erpen, W.T. Yao, B. Milke, M. Antonietti, Chem. Mater. 21 (2009) 5136–5144.
[19] K. Dewangan, S.S. Patil, D.S. Joag, M.A. More, N.S. Gajbhiye, J. Phys. Chem. C 114 (2010) 14710–14715.
[20] K.H. Lee, Y.W. Lee, A.R. Ko, G.Z. Cao, K.W. Park, J. Am. Ceram. Soc. 96 (2013) 37–39.
[21] Z.C. Li, Y. Li, E.S. Zhan, N. Ta, W. Shen, J. Mater. Chem. A 1 (2013) 15370–15376.
[22] M.J. Ledoux, C.P. Huu, J. Guille, H. Dunlop, J. Catal. 134 (1992) 383–398.
[23] M. Nagai, Y. Goto, A. Irisawa, S. Omi, J. Catal. 191 (2000) 128–137.
[24] C.H. Jaggers, J.N. Michaels, A.M. Stacy, Chem. Mater. 2 (1990) 150–157.
[25] K. Kaneda, T. Mitsudome, T. Mizugaki, K. Jitsukawa, Molecules 15 (2010) 8988–9007.
[26] S.W. Yang, C. Li, J. Xu, Q. Xin, Chem. Commun. (1997) 1247–1248.
[27] Z.L. Wu, C. Li, Z.B. Wei, P.L. Ying, Q. Xin, J. Phys. Chem. B 106 (2002) 979–987.
[28] Z.L. Wu, C. Li, P.L. Ying, Z.B. Wei, Q. Xin, Chem. Commun. (2001) 701–702